Optimum Reception in an Impulsive Interference Environment—Part I: Coherent Detection

ARTHUR D. SPAULDING AND DAVID MIDDLETON, FELLOW, IEEE

Abstract—Because communications systems are seldom significantly interfered with by classical white Gaussian noise, it is necessary to consider other, appropriate (and tractable) interference models, if realistic estimates of system performance are to be obtained for the general spectral-use environment. For this purpose, Middleton's recently developed canonical statistical-physical model of "impulsive" interference is applied to real-world communication channels. The principal features of this model are first summarized, including the statistical relations required for the solution of signal detection problems. [Excellent agreement of these model statistics with correspondingly measured statistics is also noted.]

The model for narrow-band impulsive interference (Class A noise, a subset of the overall model) is next specifically applied to an important class of coherent signal detection problems. Algorithms for error probabilities in optimum detection are then obtained, along with performance bounds, for the same error probabilities. Since it is known that in order to gain significant improvement over current receivers, the number of (essentially) independent samples of the received interference waveform must be enlarged (i.e., large "processing gains"), the performance results here are given parametrically in the number of samples, or equivalently, in the time-bandwidth product. Performance of current suboptimum receivers is then obtained and compared to the optimum performance. It is shown that very substantial savings in signal power and/or spectrum space can usually be achieved by using the indicated optimal algorithms.

Since physical realization of the completely optimum detection algorithms cannot, in general, be economically realized, the somewhat more conservative, corresponding locally optimum Bayes detection (LOBD) receivers are derived. In general, these LOBD structures require adaptive, highly non-linear filters, preceding the conventional correlation detector elements characteristic of optimum receivers for Gaussian interference. Performance for these non-linear, optimum threshold systems is then determined, specifically in Part I for coherent reception.

I. INTRODUCTION

MAN-MADE electromagnetic interference (or noise) has become a problem of great concern in the telecommunications community, particularly in the face of limited available bandwidth resources [1]. Such noise is also, and will become more and more so, a major limiting factor in the successful functioning of communication systems. There is now general recognition of the heavy price that is being paid for the effects of man-made noise on system performance. The sources of such noise are virtually unlimited—incidental radiation from electrical devices of all sorts; complex out-of-band modulation products from radio communication systems, particularly where many independent users are crowded into small geographical areas; spurious emissions from radio frequency generators of various types; minor lobe radiation from directional antennas; and so on.

The man-made EM environment, and much of the natural one as well, is basically "impulsive"; i.e., has a highly structured form, characterized by significant probabilities of large interference levels, unlike the normal noise processes inherent in transmitting and receiving elements. This impulsive, or structured character of the interference can drastically degrade the performance of conventional systems, which are designed to operate most effectively against the usually assumed normal background noise processes.

Earlier work has almost entirely focused on empirical or semi-empirical noise models, suboptimum reception, and various ad hoc approaches peculiar to the special problems under investigation. [See Sec. 1 of [2], Sec. 2 of [3], and Sec. 1.2 of [4].] The present paper, however, is devoted to the evaluation of the performance of both optimum and conventional receivers in a broad class of such "impulsive" (mostly man-made) electromagnetic interference for which a canonical, statistical-physical model has recently been constructed and experimentally verified [2], [4]. In addition, this model not only avoids the limitations of previous models but also remains tractable for the analysis required here. Specifically, of this general model only Class A interference* is considered here, when both general narrow-band and standard digital signal communications, coherently received (Part I), are employed.

A variety of important new results is obtained. These results fall principally into two categories:

(1). Canonical structures of optimum signal processors in Class A EM-environments;

(2). General performance bounds for such processors and explicit performance estimates for similar, conventional (suboptimum) receivers for the same communication tasks, and similar specific digital modems.

The technical significance of these results stems directly from the fact that one now has a general and explicitly quantitative basis for system design and comparison in the predominantly real, *non-Gaussian* (EM) interference environment, man-made or natural. Among the important results of this

Paper approved by the Editor for Communication Theory of the IEEE Communications Society for publication after presentation at the URSI General Assembly, Lima, Peru, August 1975; the URSI/USNC/IEEE/APS Annual Meeting, Boulder, CO, October 1975; the 4th International Symposium on Information Theory, Repino, Leningrad, USSR, June 1976; and the 2nd Symposium on Electromagnetic Compatibility, Montreux, Switzerland, June 1977. Manuscript received October 4, 1976; revised April 11, 1977. This work was supported in part by the OT/ITS, DoD, and OTP and represents portions of a dissertation submitted by A. D. Spaulding to the Department of Electrical Engineering, University of Denver, Denver, CO, May 1975 in partial fulfillment of the requirements for the Ph.D. degree.

A. D. Spaulding is with the Office of Telecommunications, Institute for Telecommunication Sciences, U.S. Department of Commerce, Boulder, CO 80302.

D. Middleton is at 127 E. 91 St., New York, NY 10028 under contract to the Office of Telecommunications, Institute for Telecommunication Sciences, U.S. Department of Commerce.

*Class A interference is characterized by a bandwidth comparable to or less than that of the receiver. See Section II for a more precise description of Class A noise.

Authorized licensed use limited to: University of Missouri Libraries. Downloaded on April 02,2024 at 15:40:49 UTC from IEEE Xplore. Restrictions apply.

IPR2024-00817
Apple EX1035 Page 1

analysis are the prediction of sizable spectral savings potentially available when optimum receivers are employed. In addition, such results provide essential assistance in the design and application of the measuring equipment needed for other important tasks of spectral management, viz, assessment of spectrum usage, as well as the determination and the quantitative (statistical) evaluation of the general EM environments of urban and other geographical regions. We emphasize that it is the quantitative interplay between experimentally verified, analytical model building of the electromagnetic environment and the evaluation of system performance which provides essential tools for prediction of performance, the development of adequate and appropriate data bases, standardization, and spectral assessment needed for effective management of the spectral-use environment. We also emphasize the importance of the canonical nature of the results: the *form* of optimum system structure and the analytical character of performance evaluation (error probabilities) are independent of the explicit noise statistics and signal waveforms.

Corresponding to the above discussion, this paper is organized as follows: Section II summarizes the pertinent features of Middleton's Class A impulsive interference model, including the statistics required for the present general class of signal detection problems [2, 4] and comparisons of these statistics with experiment. In Section III, we develop optimum detection algorithms and obtain exponentially tight bounds on the performance of the optimum coherent detector. In Section IV, the performance of current suboptimum (but optimum for Gaussian noise) detectors is obtained and compared with the optimum performance in these highly non-Gaussian noise environments. Since the fully optimum detector for all input signal levels is difficult to realize physically, we devote Section V to obtaining the corresponding optimum coherent threshold detectors (i.e., locally optimum Bayes detectors or LOBD's) and evaluating their performance. Finally, Section VI completes Part I with a short summary and discussion of the principal results.

II. THE IMPULSIVE INTERFERENCE MODEL (CLASS A NOISE)

In order to determine the optimum receiving system for a given class of signals and analyze its performance, a mathematical model for the random interference process is required. That is, for optimal system studies and also for determining the performance of some of the existing suboptimum systems, more information about the interference process is required than can generally be obtained by measurement alone. The interference process as seen by the receiver is, for almost all cases of interest, a narrowband process in that it can be characterized by an envelope and a phase. Narrowband noise processes arise whenever the receiver bandwidth is substantially less than the receiver center frequency. The problem is to develop a model for the interference that fits all the available measurements; is physically meaningful when the nature of the noise sources, their distributions in time and space, propagation, etc., are considered; is *directly* relatable to the physical mechanisms giving rise to the interference; and is still simple enough so that the required statistics can be obtained for solving signal detection problems. While various models have been proposed in the past which meet these requirements in particular instances, the only general (canonical) model available to date which meets all the above requirements is that which has recently been proposed by Middleton [2, 4].

For this general model we need first to distinguish between two classes of interference:

Class A: Interference arising from sources whose emission spectra are comparable to or narrower than the bandpass of our receiver (to be termed "narrowband interference"), and

Class B: Interference arising from sources whose emission spectra are broader than the bandpass of our receiver (to be termed "broadband interference").

[More precise analytic definitions are given in Section 7 (Part II) of Ref. [4].]

Both classes produce "narrowband" (i.e., envelope and phase) interference in the receiver. [We can also, of course, consider a Class C interference, defined as one which is composed of the sum of Class A and Class B components.] Examples of Class A interference include collections of unwanted signals (unwanted by our receiver, but wanted by someone else) and (depending on our receiver bandwidth, of course) the emissions of various man-made devices (e.g., radio frequency dielectric heaters, soldering machines, plastic welders, etc.). Examples of Class B interference include atmospheric noise, automotive ignition noise, arc welders, etc. Most models proposed in the past have considered only cases of Class B interference. The exception to date is Middleton's general model, which includes both Class A and Class B noise as important special cases. Here, however, we shall consider only the Class A cases. [For a full account of both Class A and B types, see [4], which gives the general analysis.]

Let us now briefly summarize the main results of the model, emphasizing the Class A component, which are needed in the solution of the various signal detection and system performance problems treated in this paper. This model is the only general one available to date in which the parameters of the model are determined *explicitly* by the underlying physical mechanisms (e.g., source density, beam-patterns, propagation conditions, emission waveforms, etc.). It is also the first model which treats narrowband input interference processes (Class A) as well as the traditional broadband input processes (Class B). As we shall see, the model is also canonical in nature, in that the analytical forms of the results do not change with changing physical conditions. We include here also some comparisons of the model with measurements for Class A cases. [Comparisons involving Class B interference are presented in Section 2.4 of Ref. [4].]

As in earlier models, the present model postulates the familiar Poisson mechanism for the initiation of the interfering signals that comprise the received waveform $X(t)$. The received interfering process is represented by

$$X(t) = \sum_j U_j(t, \theta), \tag{1}$$

Authorized licensed use limited to: University of Missouri Libraries. Downloaded on April 02,2024 at 15:40:49 UTC from IEEE Xplore. Restrictions apply.

IPR2024-00817
Apple EX1035 Page 2

where U_j denotes the jth received waveform from an interfering source and θ represents the random parameters which describe the waveform scale and structure. It is next assumed that only one type of waveform, U, is generated, with variations in the individual waveforms taken care of by appropriate statistical treatment of the parameters θ.

With the assumption that the sources are Poisson-distributed in space and emit their waveforms independently according to the Poisson distribution in time, the first-order characteristic function of $X(t)$ is well known to be [5]

$$F_1(i\xi, t)_p = \exp\left[\int_\Lambda \langle \rho(\lambda) e^{i\xi U(t;\lambda,\theta)} - 1\rangle_\theta \, d\lambda\right], \qquad (2)$$

where λ are the coordinates of the source-receiver geometry and Λ is the physical domain in which the sources are located. The $\rho(\lambda)(\geqslant 0)$ is the process density, cf. [2]. The quantity $\int_\Lambda \rho(\lambda) d\lambda \equiv A$ is one of the basic parameters of the model and $\int_\Lambda \rho(\lambda)(\cdot) d\lambda$ is a "counting" functional which adds up the contributions of the individual sources. The quantity A is called the *Impulsive Index*. Specifically, A can be shown to be equal to $\nu_T \bar{T}_s$, where ν_T is the average rate of "signal" generation and $\bar{T}_s$ is the mean duration of a typical interfering signal. The Impulsive Index measures the amount of temporal overlap among the waveforms of the interfering signals (inside the receiver). Large A means large overlap with a corresponding approach to Gauss, while small A means highly "impulsive" or structured interference.

The next step is to obtain the generic waveform $U(t)$ explicitly from the underlying physical mechanisms (see [6] for this development). The waveform $U(t)$ is written in envelope and phase form, with $B_0(t, \lambda, \theta)$ denoting the envelope. This gives us (see [1, 4])

$$F_1(i\xi)_p = \exp[\langle A J_0(B_0 \xi) - A\rangle], \qquad (3)$$

where $\langle\cdot\rangle$ denotes required statistical averages over the random epoch representing the time at which the typical jth source emits, Doppler velocities, if any, and the random signal parameters θ. The characteristic function (3) has the same form as that obtained previously by various investigators (Furutsu and Ishida [7], Giordano and Haber [8], etc.). These investigators have made various assumptions about the distributions required to perform the averages indicated in (3), have performed these averages, and have then transformed the resulting characteristic functions to obtain their models. Each different assumption, of course, leads to a different model. In our present case, we have B_0 explicitly related to the physics causing the interference. A unique approach of Middleton's model is to develop expressions for the transform of $F_1(i\xi)_p$ above without performing the indicated averages explicitly, thereby obtaining a canonical model.

For the Class A or "narrowband" interference postulated here, the signal duration T_s, inside the receiver, is finite, allowing us to write the exponent of (3) as $A\langle J_0(B_0\xi)\rangle - A$. A consequence of the above is that for the purely Poisson process, Class A noise yields "gaps in time"; i.e., non-zero probability of periods of time during which there is no interference in the receiver.** A more general model of the man-made noise environment includes an additive, independent Gaussian background process. This additive background is attributable either to receiver noise, or to the limit of a high density Poisson process representing the contributions of the nonresolvable background sources, or to both. In this case we have for the (1st-order) characteristic function of the sources process

$$F_1(i\xi)_{p+G} = F_1(i\xi)_p F_1(i\xi)_G, \qquad F_1(i\xi)_G = e^{-\xi^2 \sigma_G{}^2/2}. \qquad (4)$$

It is found [Section 3, [4]] after an appropriate steepest-descent modification of the exponent of (3), that Eq. (4) can be approximated canonically by

$$F_1(i\xi)_{P+G} \approx e^{-A} \sum_{m=0}^{\infty} \frac{A^m}{m!} e^{-c_m{}^2 \xi^2/2},$$

$$c_m{}^2 = m\langle B_0{}^2\rangle/2 + \sigma_G{}^2. \qquad (5)$$

We now define the second basic parameter of the model, Γ', as the ratio of the power in the Gaussian portion of the interference to the power in the Poisson component, viz,

$$\Gamma' \equiv \langle X_G{}^2\rangle/\langle X_p{}^2\rangle = \frac{\sigma_G{}^2}{\Omega_{2A}}; \qquad \Omega_{2A} \equiv \frac{A\langle B_0{}^2\rangle}{2}. \qquad (6)$$

For computational and discussion purposes generally, it is convenient to consider the standardized variable

$$z = X/\sqrt{\langle X_G\rangle^2 + \langle X_p\rangle^2}$$

Transforming (5) for the standardized variable z, we get the desired pdf

$$p_Z(z)_{P+G} \approx e^{-A} \sum_{m=0}^{\infty} \frac{A^m}{m!\sqrt{2\pi\sigma_m{}^2}} e^{-z^2/2\sigma_m{}^2}, \qquad (7)$$

where now

$$\sigma_m{}^2 \equiv \frac{c_m{}^2}{\Omega_{2A}(1+\Gamma')} = \frac{m/A + \Gamma'}{1+\Gamma'}. \qquad (8)$$

Note that $p_Z(z)$ is given by a weighted sum of Gaussian distributions with increasing variance. It is this result (7) for the pdf of the (normalized) instantaneous amplitude of the received interference process which we will use in subsequent sections here for the solution of signal detection problems. Figure 1 shows (7) for $\Gamma' = 0.001$ and various values of A. Note that for small A, p_Z exhibits large impulsive "tails" and as A

**On the other hand, for Class B or "broadband" interference, signal duration in the receiver is infinite, so that $\langle AJ_0 A\rangle$ must be considered as a whole, and there is zero probability of "gaps in time," because the receiver responses always overlap. For details, see Part II of Ref. [4].

Authorized licensed use limited to: University of Missouri Libraries. Downloaded on April 02,2024 at 15:40:49 UTC from IEEE Xplore. Restrictions apply.

IPR2024-00817
Apple EX1035 Page 3

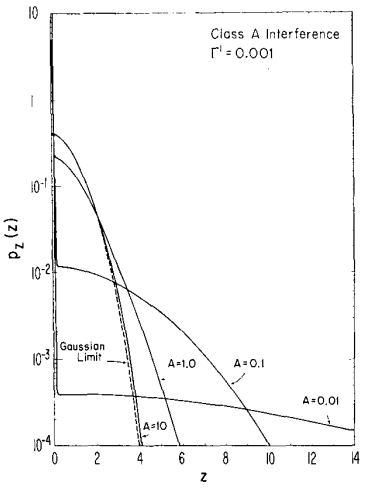

Figure 1. The pdf of the instantaneous amplitude of the interference z (Class A) for $\Gamma' = 0.001$ from (7).

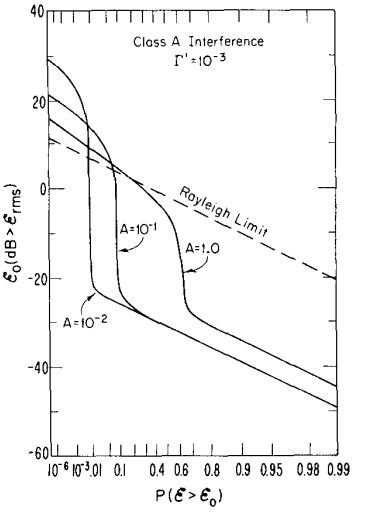

Figure 2. The envelope distribution [prob ($E > E_0$)] for Class A interference for $\Gamma' = 10^{-3}$ and various A from (9).

becomes large ($\sim$10) p_Z approaches the limiting case of Gaussian interference (still narrowband, however).

Our next step is to present the corresponding results for the envelope distribution [4]. The Class A envelope distribution is obtained from a similar expansion of the characteristic function, after averaging out the uniformly distributed phase. The result is, not surprisingly, for the standardized envelope $(=E/\sqrt{2\Omega_{2A}(1+\Gamma')})$

$$P(E > E_0)_A = e^{-A} \sum_{m=0}^{\infty} \frac{A^m}{m!} e^{-E_0{}^2/\sigma_m{}^2}; \tag{9}$$

i.e., a weighted sum of Rayleigh distributions with increasing variance. Figure 2 shows (9) for $\Gamma' = 10^{-3}$ and various values of Impulsive Index A. The coordinates used in Figure 2 are such that a Rayleigh distribution (envelope of Gauss) plots as a straight line of slope $-1/2$. Note, particularly, the impulsive "tails" departing from the low level Gaussian background at the lower probabilities.

To handle detection problems generally, we must initially formulate them on the basis of discrete random variables, which in turn are time-samples from the random process (waveform) representing the interference. For non-Gaussian situations it is also generally necessary to postulate that these random variables (samples) are effectively independent, so that only first order pdf's are needed to determine the required nth order pdf's for the sample data vectors on which the detection algorithms are based.

We first note that by assuming independent samples we obtain an *upper bound* on performance for the truly optimum detector, since if the samples were correlated, the optimum detector would make use of the information contained in this correlation to "reduce" the interference. That is, the performance of the optimum detector for correlated samples can be no worse than the performance of the optimum detector for uncorrelated samples (for the same continuous detection time from which the discrete samples are taken). [Reference [3] gives some reasonable criteria for what constitutes "effectively" independent samples for Class A interference.]

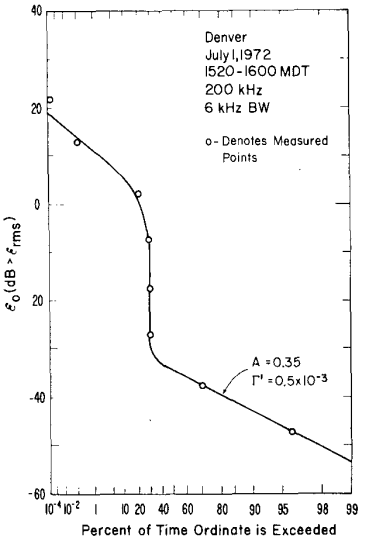

Figure 3. Comparison of measured envelope distribution (from Bolton [14], narrowband interference) with the Middleton model [4], Class A, distribution (9).

To complete our brief account of the needed first-order statistics of Middleton's Class A interference model [cf. Eqs. (5), (7), (9)], let us present two examples comparing the model (here Eq. (9)) with experimental data to illustrate the excellent agreement obtainable between experiment and theory.*** Figure 3 shows the measured envelope distribution, $P(E > E_0)$, of a narrowband impulsive interference (from Bolton [10], Fig. 17) along with the envelope distribution (9)

***Similar excellent agreement in the more complex Class B cases is also obtained [cf. Figs. 2.3-2.8 and Section 2.4 of Ref. [4]].

Authorized licensed use limited to: University of Missouri Libraries. Downloaded on April 02,2024 at 15:40:49 UTC from IEEE Xplore. Restrictions apply.

IPR2024-00817
Apple EX1035 Page 4

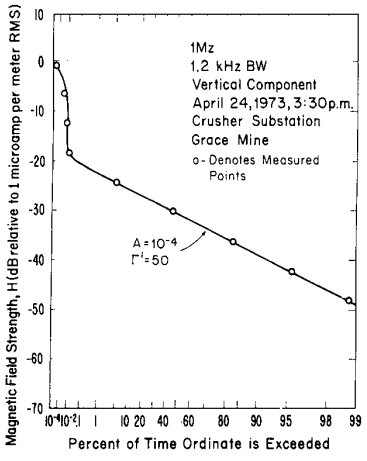

Figure 4. Comparison of measured envelope distribution (from Adams et al. [13], ore-crushing machinery) with the Middleton model [4], Class A, distribution (9).

for $A = 0.35$ and $\Gamma' = 0.5 \times 10^{-3}$. The comparison is seen to be excellent, and we will consistently use this example, when, in subsequent sections, we compute specific measures of optimum system performance. Figure 4 shows the measured envelope distribution (from Adams et al. [9], Fig. 4-17) of narrowband interference from ore crushing machinery along with the envelope distribution (9) for $A = 10^{-4}$ and $\Gamma' = 50$. Again, agreement between experiment and theory is quite excellent. Finally, we stress once more the canonical nature of these noise models: the form and structure of the distributions, *and* parameters, are invariant of any particular noise source and specific numerical values, as long as the noise is a Class A (or B) type.

III. THE OPTIMUM COHERENT RECEIVER: STRUCTURE AND PERFORMANCE

In this section we will determine the canonical structure of the optimum coherent detector and then obtain explicit bounds on its performance for the three basic classes of coherent binary digital reception, when the interfering noise is Class A interference; i.e., where the emission bandwidths of the interferers are (comparable to or) less than that of the receiver [cf. Section II preceding].

The problem of obtaining an optimum decision algorithm is well-known to be one of simple-hypothesis testing here, following the Bayes' strategy (Part IV, Ref. [3]). We have the two hypotheses classes:

$$H_1: X(t) = S_1(t) + Z(t), \qquad 0 \leqslant t < T$$
$$H_2: X(t) = S_2(t) + Z(t), \qquad 0 \leqslant t < T, \tag{10}$$

where $X(t)$ is our received waveform, $S_1(t)$ or $S_2(t)$ is the desired signal completely known at the receiver, $Z(t)$ is the interference process (here Class A noise) and $(0, T)$ is the observation period ($\equiv$ sample duration).

For the explicit portions of the analysis, we shall consider the three basic signal sets;

(i). *antipodal signals:*

$$S_1(t) = \sqrt{2S}\cos(\omega_0 t), \qquad 0 \leqslant t < T$$
$$S_2(t) = -\sqrt{2S}\cos(\omega_0 t), \qquad 0 \leqslant t < T, \tag{11}$$

(ii). *orthogonal signals:*

$$S_1(t) = \sqrt{2S}\sin(\omega_0 t), \qquad 0 \leqslant t < T$$
$$S_2(t) = \sqrt{2S}\cos(\omega_0 t), \qquad 0 \leqslant t < T, \tag{12}$$

(iii). *and ON-OFF keyed signals:*

$$S_1(t) = \sqrt{2S}\cos(\omega_0 t), \qquad 0 \leqslant t < T$$
$$S_2(t) = 0, \qquad 0 \leqslant t < T, \tag{13}$$

where $\omega_0 T \gg 1$, and S is the signal power.

We can represent (10) in vector form

$$X = S_j + Z, \qquad j = 1, 2, \tag{14}$$

where X is a vector of N samples of our received waveform $X(t)$, $x_n = X(t_n)$, and we assume that the sample times $\{t_n\}$ are such that the noise samples $\{z_n\}$ are statistically independent. The consequences of this postulation of independence have been discussed in Section II above.

Now, for the optimum (i.e., Bayes or minimum average risk) detection strategy chosen here, the optimum test statistic is well known to be the likelihood ratio $\Lambda_n(X) = q_2 P_n(X \mid H_2)/q_1 P_n(X \mid H_1)$, cf. [11]. In the present Bayes test, we set the a priori probabilities of transmission $q_1 = q_2 = 1/2$, and the threshold $K = 1$. This is the usual situation in digital transmission systems and, in any case, all the results of this section can be easily and directly modified for arbitrary K(and q_1, q_2). Then the canonical form of the likelihood ratio for our case of coherent reception in Class A noise, with the assumption of independent samples, is explicitly with the decision process,

$$\Lambda(X) = \frac{\prod_{n=1}^{N} \sum_{m=0}^{\infty} e^{-A} \frac{A^m}{m!\sqrt{2\pi\sigma_m^2}} e^{-(x_n - s_{2n})^2/2\sigma_m^2}}{\prod_{n=1}^{N} \sum_{m=0}^{\infty} e^{-A} \frac{A^m}{m!\sqrt{2\pi\sigma_m^2}} e^{-(x_n - s_{1n})^2/2\sigma_m^2}} \underset{H_2}{\overset{\text{decide: } H_1}{\gtrless}} 1, \tag{15}$$

where s_{1n} and s_{2n} are samples of the signals $S_1(t)$ and $S_2(t)$ and x_n are the samples of our received waveform.

The likelihood ratio (15) cannot in general be simplified further. We will show later [Section V] how a small-signal assumption can be used, which greatly reduces the complexity of (15), to yield a physically realizable receiver which is optimum for threshold (i.e., suitable small) signals, but which in general becomes suboptimum at the higher signal levels. The data processing (on-line or off) required of a receiver of the

Authorized licensed use limited to: University of Missouri Libraries. Downloaded on April 02,2024 at 15:40:49 UTC from IEEE Xplore. Restrictions apply.

IPR2024-00817
Apple EX1035 Page 5

type (15) is straightforward but lengthy (viz. (15)). However, it is usually uneconomical to build such a receiver, when much simpler and satisfactory threshold devices can be constructed.

Our next step is to compute the performance of the optimum (theoretical) receiver specified by (15). For this purpose we shall exploit a number of recent results involving probability bounds. We start by noting that Hellman and Raviv [12] make the elegant observation that the average probability of error in any binary communication channel ($K = 1$) is given by

$$P_e = \int_X \min \{q_1 p(X \mid H_1), q_2 p(X \mid H_2)\}\, dX, \tag{16}$$

where the integral sign with a bar denotes a multidimensional integral (N dimensions). The above cannot be attacked directly for large N because of the high dimensionality and because the regions of integration are quite awkward. However, we can use the inequality

$$\min \{a, b\} \leqslant a^{\alpha} b^{1-\alpha}, \tag{17}$$

for all $0 \leqslant \alpha \leqslant 1$, $a \geqslant 0$, $b \geqslant 0$, to obtain ($K = 1$)

$$P_e \leqslant q_1{}^{\alpha} q_2{}^{1-\alpha} \int_X [p(X \mid H_1)]^{\alpha} [p(X \mid H_2)]^{1-\alpha}\, dX. \tag{18}$$

The inequality (18) is valid for any α, $0 \leqslant \alpha \leqslant 1$, but we desire a tight upper bound. That is, we wish to use that value of α, namely α^*, which minimizes the right-hand side of (18). In the one-dimensional case, the use of $\alpha = \frac{1}{2}$ gives the Bhattacharyya bound (Sec. 2.7, Van Trees [13] and the use of α^* gives the Chernoff bound (Sec. 2.7, Van Trees [13]. The usual procedure is to obtain the Chernoff bound via the moment generating function for the one-dimensional case. Next, to assume all signal samples are the same, so that if β is the bound for $N = 1$, β^N is the bound for N samples (see, for example, Hall [14] and Spaulding et al. [15]).

This procedure does not necessarily correspond to the actual physical signals we have chosen, however. In our case, since $q_1 = q_2 = 1/2$, we have

$$P_e \leqslant \frac{1}{2} \int_{-\infty}^{\infty} \left[\prod_{n=1}^{N} \sum_{m=0}^{\infty} e^{-A} \frac{A^m}{m!\sqrt{2\pi\sigma_m{}^2}} \cdot e^{-(x_n - s_{1n})^2/2\sigma_m{}^2} \right]^{\alpha} \cdot \left[\prod_{n=1}^{N} \sum_{m=0}^{\infty} e^{-A} \frac{A^m}{m!\sqrt{2\pi\sigma_m{}^2}} \cdot e^{-(x_n - s_{2n})^2/2\sigma_m{}^2} \right]^{1-\alpha} d\boldsymbol{x}, \tag{19a}$$

and we are interested in large N. Equation (19a) reduces to

$$P_e \leqslant \frac{1}{2} \prod_{n=1}^{N} \int_{-\infty}^{\infty} \left[\sum_{m=0}^{\infty} e^{-A} \frac{A^m}{m!\sqrt{2\pi\sigma_m{}^2}} \cdot e^{-(x_n - s_{1n})^2/2\sigma_m{}^2} \right]^{\alpha} \cdot \left[\sum_{m=0}^{\infty} e^{-A} \frac{A^m}{m!\sqrt{2\pi\sigma_m{}^2}} \cdot e^{-(x_n - s_{2n})^2/2\sigma_m{}^2} \right]^{1-\alpha} dx_n. \tag{19b}$$

Let

$$\rho_n = \frac{s_{1n} - s_{2n}}{2} \text{ and } y = x_n - \frac{s_{1n} + s_{2n}}{2}. \tag{20}$$

Now we can write the canonical result (independent of the particular signal waveforms and noise parameters employed):

$$P_e \leqslant \frac{1}{2} \prod_{n=1}^{N} I_{\alpha}(\rho_n), \tag{21a}$$

where

$$I_{\alpha}(\rho_n) = \int_{-\infty}^{\infty} \left[\sum_{m=0}^{\infty} e^{-A} \frac{A^m}{m!\sqrt{2\pi\sigma_m{}^2}} \cdot e^{-(y-\rho_n)^2/2\sigma_m{}^2} \right]^{\alpha} \cdot \left[\sum_{m=0}^{\infty} e^{-A} \frac{A^m}{m!\sqrt{2\pi\sigma_m{}^2}} \cdot e^{-(y+\rho_n)^2/2\sigma_m{}^2} \right]^{1-\alpha} dy. \tag{21b}$$

We require that

$$I_{\alpha^*}(\rho_n) = \inf_{0 \leqslant \alpha \leqslant 1} I_{\alpha}(\rho_n). \tag{22}$$

Now we know that $I_{\alpha}(\rho_n)$ is convex U on [0, 1] (Hellman and Raviv, [12]), and we see that the integral in (21b) is symmetrical about $\alpha = 1/2$. Therefore, $\alpha^* = 1/2$. Our task has now been reduced to the computation of the single integral in (21b) with $\alpha = 1/2$. [We also note that for any α, $I_{\alpha}(0) = 1$.] This integral can be evaluated, for arbitrary ρ_n, only by numerical techniques. Looking at Figure 1, we see that the integral is not particularly well behaved in the neighborhood of $y = \rho_n$, and that the normal Gaussian quadrature approach to infinite integrals does not apply. We use an adaptive Romberg quadrature developed to handle integrands of our type (Miller [16]).

Figure 5 shows $I_{1/2}(\rho_n)$, $\rho_n \geqslant 0$, for two cases: $A = 0.35$, $\Gamma' = 0.5 \times 10^{-3}$ (cf. Fig. 3) and $A = 0.1$, $\Gamma' = 10^{-3}$. Our bound on performance can now be obtained from (21a). In order to use (21a) for large N, we require specific signal samples, ρ_n, and a means of obtaining the values of $I_{1/2}(\rho_n)$ for

Authorized licensed use limited to: University of Missouri Libraries. Downloaded on April 02,2024 at 15:40:49 UTC from IEEE Xplore. Restrictions apply.

IPR2024-00817
Apple EX1035 Page 6

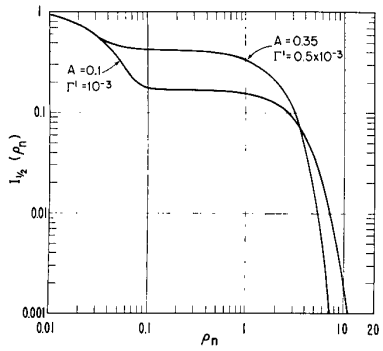

Figure 5. The integral $I_{1/2}(\rho_n)$, (21b) for two example cases along with the upper bound $\hat{I}_{1/2}(\rho_n)$, (25).

each ρ_n. This is done as follows for our three signal sets (11), (12), and (13). We let

$$t_n = \frac{T}{N-1}(n-1); \qquad 1 \leqslant n \leqslant N \text{ and } Q = \omega_0 T. \tag{23}$$

We obtain, then, from (20) and (11) through (13),

$$\rho_n = \sqrt{2S}\cos\left[\frac{Q}{N-1}(n-1)\right], \text{ antipodal,}$$

$$\rho_n = \sqrt{S}\cos\left[\frac{Q}{N-1}(n-1) - \frac{3\pi}{4}\right], \text{ orthogonal,}$$

$$\rho_n = \sqrt{S/4}\cos\left[\frac{Q}{N-1}(n-1)\right], \text{ ON-OFF keyed,} \tag{24}$$

where for the ON-OFF keyed system, we have also followed the convention of using the average signal power in the two signals S_1, S_2, cf. (13); i.e., one-half the power of either signal in the other cases.

We next develop a simple upper bound, $\hat{I}_{1/2}(\rho_n)$, to $I_{1/2}(\rho_n)$, which can be quickly evaluated by the computer. For the case $A = 0.35$, $\Gamma' = 0.5 \times 10^{-3}$ (cf. Fig. 3), we use

$$\left.\begin{aligned} \hat{I}_{1/2}(\rho_n) &= 0.42 + 0.58e^{-1200\rho_n^2}, && 0 \leqslant |\rho_n| \leqslant 0.1 \\ \hat{I}_{1/2}(\rho_n) &= 0.42e^{-0121|\rho_n|^{1.69}}, && |\rho_n| > 0.1. \end{aligned}\right\} \tag{25}$$

The expression (25) is obtained by adjusting (via a computer) functions of the form $K_1 \exp K_2 |\rho_n|^{K_3}$ until a tight upper bound is achieved. This bound for $I_{1/2}(\rho_n)$ is also shown on Figure 5, but cannot be distinguished from $I_{1/2}(\rho_n)$. Now, with the help of (24) and (25), we find that our desired tight upper bound on performance, $\hat{P}_e$, is given by

$$P_e \leqslant \hat{P}_e = \frac{1}{2}\prod_{n=1}^{N} \hat{I}_{1/2}(\rho_n) \tag{26}$$

and we now use S for the SNR for the antipodal and orthogonal systems and $S/2$ for the SNR for the ON-OFF system. (Since the noise has been normalized, average noise power = 1.)

By varying the parameter Q we change the number of oscillations of our desired signal in the detection period T. Extensive calculations (see Spaulding and Middleton [3]) have shown that performance is only weakly dependent on Q.

Figure 6 shows results for the three signal types (11-13), (26) for $Q = 10$ and $N = 10$; and Figure 7, similarly, for $Q = 100{,}000$ and $N = 100$. Figure 8 gives results for the ON-OFF systems for $Q = 1000$ and various sample sizes $N = 10$, 100, and 1000. We note that, as it should, the probability of error P_e approaches zero as (independent) sample size N becomes large. That is, we can make P_e as small as we like by making sample-size N large enough, which corresponds to making T large, or equivalently, by making the time-bandwidth product ($\approx N$) large.

As we have noted earlier (Eq. (7) et seq.), when the Impulsive Index A becomes large ($\geqslant 10$), our interference distribution approaches the Gaussian. The coherent receiver which is optimum for Gauss is the well-known correlation or "matched-filter" receiver (if we assume appropriate pre-whitening, since we are still dealing with narrow-band interference). Performance is given in terms of the signal energy, E (cf. Eqs. 4.51, 4.38, Ref. [3]) and the correlation, ϕ, between $S_1(t)$ and $S_2(t)$, viz.,

$$P_e = \frac{1}{2}\operatorname{erfc}\sqrt{\frac{E(1-\phi)}{2}}, \tag{27}$$

where erfc denotes the complimentary error function. Here $\phi = -1$ for antipodal signals and $\phi = 0$ for orthogonal signals and ON-OFF keying. For the performance bound (21a) we easily obtain

$$P_e \leqslant \frac{1}{2}\exp[-E/k], \tag{28}$$

with $k = 1$ for antipodal, 2 for orthogonal, and 4 for the ON-OFF system. Figure 9 shows (27) and (28) for this Gaussian interference case.

IV. PERFORMANCE OF COHERENT SUB-OPTIMUM RECEIVERS

The receivers in general use today are basically those designed to be optimum when the interference is white Gaussian noise. These are the well-known correlation, or "matched filter" receivers (Hancock and Wintz [19]). In this section the expected performance of these receivers subject to the (highly) non-Gaussian Class A interference is determined, and this performance is then compared with that of the corresponding optimum detector derived and analyzed earlier [cf. Section III].

We can obtain the performance of the correlation receiver most easily by using a geometric representation of the receiving system (see Arthurs and Dym [20]). Using this approach, Halton and Spaulding [21] have analyzed the performance of differentially coherent phase (shift-keyed) systems (DCPSK) in impulsive noise. The performance of these three systems [correlation detectors, a class of the optimum coherent systems of Section III, and the DCPSK systems] can be obtained from

Authorized licensed use limited to: University of Missouri Libraries. Downloaded on April 02,2024 at 15:40:49 UTC from IEEE Xplore. Restrictions apply.

IPR2024-00817
Apple EX1035 Page 7

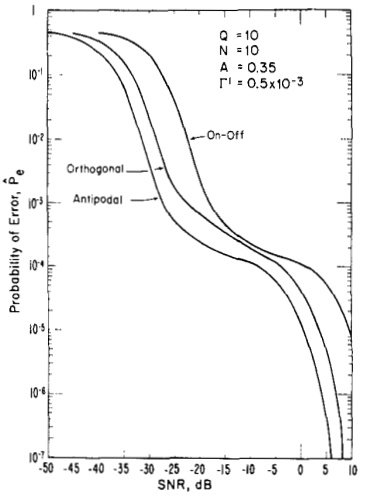

Figure 6. The upper bound on performance, $\hat{P}_e$, (26) for the three signaling cases (24) for $N = 10$ independent samples and $Q = 10$.

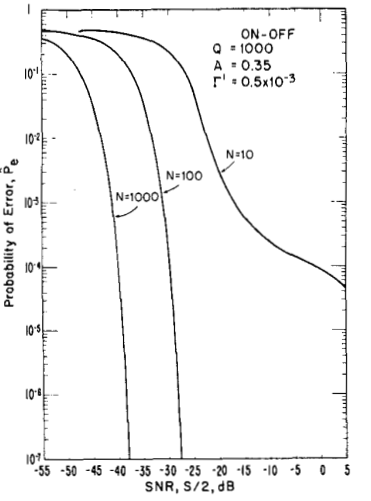

Figure 8. The upper bound on performance, $\hat{P}_e$, (26) for the ON-OFF signaling case for $Q = 1000$ and $N = 10$, 100, and 1000, the number of independent samples.

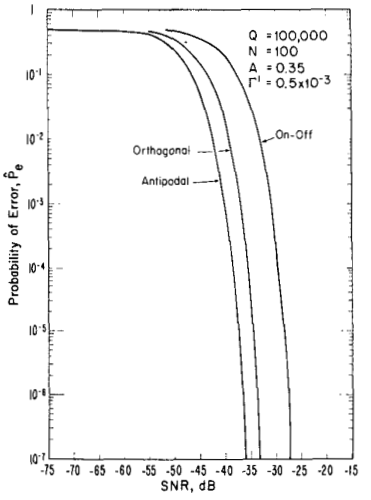

Figure 7. The upper bound on performance, $\hat{P}_e$, (26) for the three signaling cases (24) for $N = 100$ independent samples and $Q = 100{,}000$.

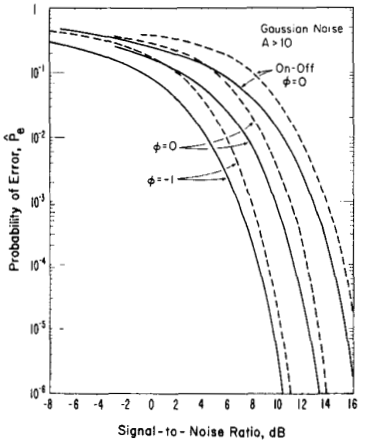

Figure 9. Comparison of theoretical performance in Gaussian noise (from (27)) and the upper bound (28) (dashed curves).

these results, since antipodal signaling produces a binary coherent phase shift-keying (CPSK), which is a special case of the multilevel DCPSK results. We find, using (24) of Halton and Spaulding [21], that, in general, for binary CPSK, the average probability of error is given by

$$P_e = \frac{1}{\pi}\int_{\sqrt{S}}^{\infty} p(E)\cos^{-1}\left(\frac{\sqrt{S}}{E}\right)dE, \tag{29}$$

where $p(E)$ is the probability density of the noise *envelope* voltage, normalized to the rms noise and, where as before, the SNR is given by S.

The cumulative distribution of the envelope of Class A interference is given by Eq. (9) and the associated pdf by the negative of the derivative of (9). Using this in (29), interchanging integration and summation, integrating by parts, and making a change of variable, we obtain

$$P_e = e^{-A}\sum_{m=0}^{\infty}\frac{A^m}{m!}\frac{e^{-S/\sigma_m^2}}{\pi}\int_0^{\infty}\frac{e^{-Sy^2/\sigma_m^2}}{y^2+1}dy,$$

which gives us, finally,

$$P_e = \frac{e^{-A}}{2}\sum_{m=0}^{\infty}\frac{A^m}{m!}\operatorname{erfc}\sqrt{S/\sigma_m^2}. \tag{30}$$

The result (30) applies for binary CPSK. In general, from the geometrical representation of the correlation receivers, [21], this gives immediately

$$P_e = \frac{e^{-A}}{2}\sum_{m=0}^{\infty}\frac{A^m}{m!}\operatorname{erfc}\sqrt{S/k\sigma_m^2}, \tag{31}$$

where $k = 1$ for antipodal signals, $k = 2$ for orthogonal signals,

Authorized licensed use limited to: University of Missouri Libraries. Downloaded on April 02,2024 at 15:40:49 UTC from IEEE Xplore. Restrictions apply.

IPR2024-00817
Apple EX1035 Page 8

and $k = 4$ for OFF-ON keying. Figure 10 shows the calculated performance, from (30) for antipodal signals for $\Gamma' = 1 \times 10^{-4}$, parametric in A. There have been few measurements of the performance of these receivers in narrow-band interference, however. Some measurements of Mayer [22] for receiver performance in various types of interfering signals, while not directly corresponding to the Class A model, show results very similar to those calculated (Fig. 10) here for this narrow-band interference [see Fig. 4.10 of [3]]. Other analyses of suboptimum receiver performance, i.e., for appropriate types of correlation detectors, in Poisson noise (essentially Class B and quantitatively for coherent FSK only), have been carried out recently by Corti et al. [17], [18].

We wish now to compare the performance of these suboptimum systems with that of our optimum system [Sec. III]. Figure 11 shows the performance of the optimum receiver compared with the theoretical performance of the standard correlation receiver for antipodal signaling with the two sample sizes $N = 10$ and 100. Our data example [Fig. 3], with parameter $A = 0.35$, $\Gamma' = 0.5 \times 10^{-3}$, is used. For this system, $N = 10$ corresponds to a time-bandwidth product 10. We note that the optimum system does not perform much better than the current suboptimum system for this time-bandwidth product, when very small error probabilities (very small P_e) are required. For $N = 100$, however, we see that the optimum system performs substantially better than the correlation receiver, for the same time-bandwidth product. For example, these results indicate that if a time-bandwidth product 100 is used to combat interference (a not unusual situation), then the optimum system requires at least 33 dB *less* signal power than the correlation receiver to achieve an error rate of 10^{-5} or less. Another way of looking at this is in terms of usage of the spectrum resource. These results (Fig. 11) indicate that for a given signal power and performance criterion ($P_e = 10^{-5}$, say), the optimum system can achieve this performance with a time-bandwidth product somewhere between 10 and 20, while the suboptimum system requires a time-bandwidth product of 100. That is, somewhere between 5 and 10 times the actual required amount of spectrum space is currently being used by the suboptimum system (in this example). [Note in Fig. 11 that for large $P_e (P_e \sim 1/2)$ the suboptimum receiver apparently performs better than the optimum receiver. This is attributable to the looseness of the upper bound used to specify optimum performance at large P_e (see Fig. 9, for example). Of course, by definition the optimum receiver must give superior performance vis-a-vis any suboptimum receiver for the same purpose under the same conditions.]

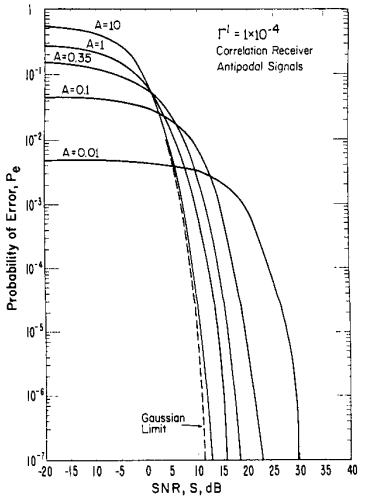

Figure 10. Performance of the correlation receiver (Gaussian optimum receiver) in Class A interference (30) for $\Gamma' = 10^{-4}$ for various values of the impulsive index A.

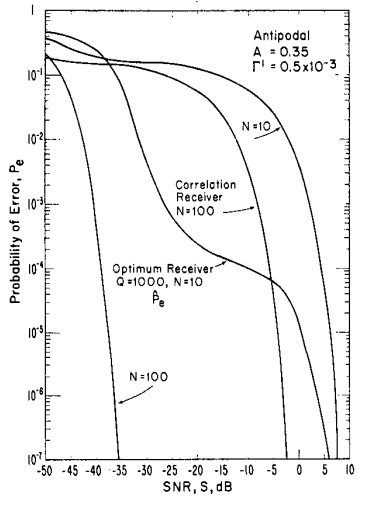

Figure 11. Comparison of performance of correlation receiver in Class A interference with the upper bound on optimum performance (26) for $Q = 1000$ and $N = 10$ and 100 for antipodal signals.

V. OPTIMUM COHERENT THRESHOLD DETECTION:

As we have seen above, even in the simplest coherent signaling cases, the optimum detector is quite difficult to realize physically, even though we were able to compute a bound on its performance. For this reason most past efforts to obtain optimum structure and performance measures have been directed to finding a detector which approaches the limiting optimum Bayes detector when threshold operations are used (namely, the LOBD ≡ locally optimum Bayes detector) i.e., when the desired signal becomes vanishingly small and the number of independent samples becomes large [so that acceptably small error probabilities result]. In this section we derive the LOBD for binary, purely coherent signals and discuss under what conditions it is asymptotically optimum.† The general problem for both coherent and incoherent reception and arbitrary additive interference was apparently first attacked by Middleton [11, 23], who showed that the optimum threshold receiver must be a nonlinear processor. Somewhat later, Rudnick [24] examined the same problem. Using a power series expansion technique similar to Middleton's, he

†In Part II following, we obtain analogous results for some forms of incoherent reception.

Authorized licensed use limited to: University of Missouri Libraries. Downloaded on April 02,2024 at 15:40:49 UTC from IEEE Xplore. Restrictions apply.

IPR2024-00817
Apple EX1035 Page 9

obtained closed forms for the nonlinear optimum receivers and showed, in addition, that they must be adaptive. Later canonical results have been obtained by Middleton [25], Antonov [26], Levin and Kushnir [27], and Levin and Shinakov [28].

Our present detection situation is to decide optimally between the two hypotheses H_1, H_2, as given by (10) earlier. The likelihood ratio (for these a priori symmetric channels, e.g., $q_1 = q_2 = 1/2$, $K = 1$, cf. Section III) and decision process are, for these additive signal and noise processes,

$$\Lambda(X) = \frac{p(X \mid H_2)}{p(X \mid H_1)} = \frac{p_Z(X - S_2)}{p_Z(X - S_1)} \underset{H_2}{\overset{\text{decide: } H_1}{\gtrless}} 1, \tag{32}$$

where $p_Z(X - S_j), j = 1, 2$ is expanded about $S_j = 0$, for threshold signals, according to

$$P_Z(X - S_j) = p_Z(X) - \sum_{i=1}^{N} \frac{\partial p_Z(X)}{\partial x_i} s_{ji} + \frac{1}{2} \sum_{i=1}^{N} \sum_{k=1}^{N} \frac{\partial^2 p_Z(X)}{\partial x_i \partial x_k} s_{ji} s_{jk} + \cdots, \tag{33a}$$

with $X = \{x_i\}$, $S_j = \{s_{ji}\}$ etc., for the component elements of received data and signals. For coherent signals, the usual small-signal assumption is

$$p_Z(X - S_j) \approx p_Z(X) - \sum_{i=1}^{N} \frac{\partial p_Z(X)}{\partial x_i} s_{ji}, \tag{33b}$$

where we have ignored all signal terms of order 2 and higher.†† Inserting (33b) into (32), dividing the numerator and denominator by $P_Z(X)$, and assuming independent noise samples (for our present analysis), we get directly

$$\Lambda(X) \approx x^* \equiv \frac{1 - \sum_{i=1}^{N} s_{2i} \frac{d}{dx_i} \ln p_Z(x_i)}{1 - \sum_{i=1}^{N} s_{1i} \frac{d}{dx_i} \ln p_Z(x_i)} \underset{H_2}{\overset{\text{decide: } H_1}{\gtrless}} 1, \tag{34}$$

for the desired LOBD structure and decision process. Since the additive constant, unity, does not affect the test, one physical implementation of the operation indicated in (34) is shown in Figure 12. We see that x^* is simply the standard coherent receiver for Gaussian noise, preceded by a logarithmic nonlinearity. This same result has been obtained by Algazi and Lerner [29] and Nirenberg [30], as well as others. The general result for coherent signals is that in order to choose the most likely signal from among the ensemble of possible received signals, the optimum threshold receiver is the standard Gaussian receiver preceded by the above nonlinearity. Note that this is a

††This small-signal assumption is really intuitive, and one needs to show that the higher order terms are not required for asymptotic optimality; cf. [25], [27], [32], [34], and [35].

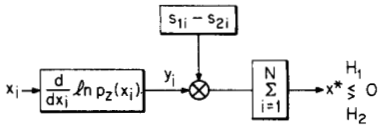

Figure 12. Locally optimum (Bayes) receiver, x^*, for purely coherent binary signals.

canonical receiver: its general form and the decision process are independent of any particular type of interference. Note, also, that this receiver must be *adaptive;* i.e., it is required to adjust itself for changing interference conditions. It must know a priori, or estimate, $p_Z(X)$. Some approximations to this receiver have been built and tested (Bernstein and McNeill [31]) for use where the impulsive interference is atmospheric noise (an example of Class B interference [4]).

For our Class A interference, Figure 13 shows the required nonlinearity, $(-d/dx)\ln p_Z(x)$, for our two examples, $A = 0.35$, $\Gamma' = 0.5 \times 10^{-3}$, and $A = 0.1$, $\Gamma' = 10^{-3}$. [We see that it can be rather difficult to implement physically.] While the nonlinearity does not "Gaussianize" the interference, it does suppress the large "spikes". Since N is large, the signal is small, and the interference has been reduced in its amplitude excursions (Fig. 13), performance can be estimated via the Central Limit Theorem. Our previous bound (26) was quite good only for small P_e [cf. Fig. 14, also]. Analyzing the performance of the above locally optimum threshold detector will, therefore, give an estimate of performance of the optimum detector for small signals and large N.

Let us start by rewriting the test (34) in the more convenient form [cf. Fig. 12].

$$x^* = \sum_{i=1}^{N} (s_{1i} - s_{2i}) \frac{d}{dx_i} \ln p_Z(x_i) \underset{H_2}{\overset{\text{decide: } H_1}{\gtrless}} 0 \tag{35}$$

Suppose $H_1: X(t) = S_1(t) + Z(t)$ is true; then we have

$$E[y_i \mid H_1] = \int_{-\infty}^{\infty} y_i p(y_i)\, dy_i = \int_{-\infty}^{\infty} dx \ln p_Z(x) p_Z(x - s_{1i})\, dx \cong \int_{-\infty}^{\infty} \frac{p_Z'(x)}{p_Z(x)} \{p_Z(x) - s_{1i} p_Z'(x)\}\, dx, \tag{36a}$$

where the small-signal assumption (33b) has again been used and y_i is the output of the nonlinearity for the input x_i. Since $p_Z'(-x) = -p_Z'(x)$ [i.e., $p_Z(x)$ is symmetric about $x = 0$], (36a) reduces to

$$E(y_i \mid H_1) \approx -s_{1i} L, \tag{36b}$$

where

$$L = \int_{-\infty}^{\infty} \left[\frac{d}{dx} \ln p_Z(x)\right]^2 p_Z(x)\, dx. \tag{36c}$$

Authorized licensed use limited to: University of Missouri Libraries. Downloaded on April 02,2024 at 15:40:49 UTC from IEEE Xplore. Restrictions apply.

IPR2024-00817
Apple EX1035 Page 10

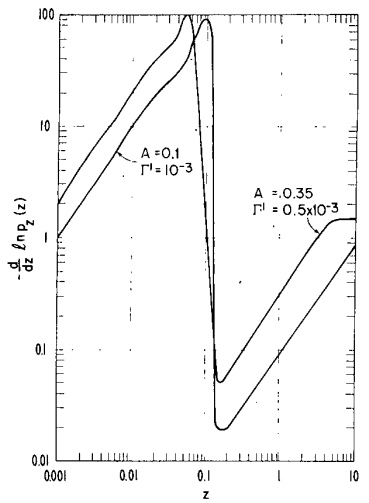

Figure 13. The nonlinearity, $-d/dx \ln p_Z(z)$, for two example cases of Class A interference.

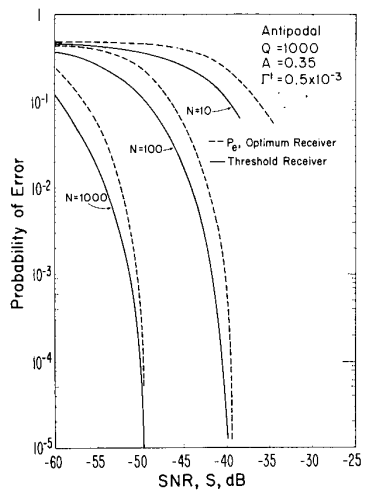

Figure 14. Comparison of the estimate of performance for small signal (42) with the upper bound on performance (26) for $Q = 1000$, $N = 10$, 100, and 1000 for antipodal signals.

Also, we have for the second moment

$$E[y_i^2 \mid H_1] = \int_{-\infty}^{\infty} \left[\frac{d}{dx} \ln p_Z(x)\right]^2 \{p_Z(x) - s_{1i} p_Z'(x)\}\, dx. \tag{37}$$

Again, since $p_Z(x)$ is even and $p_Z'(x)$ is odd, this gives us

$$E[y_i^2 \mid H_1] = L, \tag{38a}$$

$$\text{Var } [y_i \mid H_1] = L - s_{1i}^2 L^2. \tag{38b}$$

After multiplying by $s_{1i} - s_{2i}$ and summing over the N samples, we obtain the following statistics for the decision variable x^* (cf. Fig. 12), under H_1:

$$E[x^* \mid H_1] = L \sum_{i=1}^{N} (-s_{1i}^2 + s_{1i} s_{2i}),$$

$$\text{Var } [x^* \mid H_1] = \sum_{i=1}^{N} (s_{1i} - s_{2i})^2 (L - s_{1i}^2 L^2) \approx$$

$$\approx L \sum_{i}^{N} (s_{1i} - s_{2i})^2 \tag{39}$$

this last to be consistent with the coherent approximation, $0(s_i)$, cf. (33b). [Note that these results are still canonical in the signal waveform, as well as the noise statistics.]

For the particular example of Fig. 11 (and Class A data, Fig. 3), where antipodal signals are used, so that $s_{1i} - s_{2i} = 2\sqrt{2S} \cos \omega_0 t_i$, we find specifically that

$$E[x^* \mid H_1] = -4SL \sum_{i=1}^{N} \cos^2 \omega_0 t_i \approx -2SLN \tag{40a}$$

and

$$\text{Var } [x^* \mid H_1] = \sum_{i=1}^{N} (8SL \cos^2 \omega_0 t_i - 16S^2 L^2 \cos^4 \omega_0 t_i)$$

$$\approx 4SLN - 6S^2 L^2 N \approx 4SLN,$$

$$SL \ll 1, N \gg 1. \tag{40b}$$

In similar manner, we obtain

$$E[x^* \mid H_2] = -E[x^* \mid H_1], \quad \text{Var } [x^* \mid H_2] = \text{Var } [x^* \mid H_1] \tag{41}$$

By the Central Limit Theorem (CLT) for these large numbers, N, of (independent) samples, we find formally that the desired performance estimate for small signal and large N approaches

$$P_e = \text{Prob } [x^* > 0] = \frac{1}{2} \text{erfc} \left\{ \frac{|E[x^*]|}{\sqrt{2 \text{ Var } [x^*]}} \right\}$$

$$\approx \frac{1}{2} \text{erfc } (\sqrt{SLN/2}, \qquad SL \ll 1, N \gg 1. \tag{42}$$

We see at once for (40b) that S must be quite small in order for the variance to be positive in this approximation, which is to be expected from the small signal assumption, especially as used in (37). Performance is a function of S, N, and the parameter L, where L is given by (36c). For our two specific numerical examples (cf. Fig. 13) of Class A noise, the evaluation of (36c) must be carried out numerically. This gives [for $A = 0.1$ and $\Gamma' = 10^{-3}$] $L = 892.7$ [for $A = 0.35$, $\Gamma' = 0.5 \times 10^{-3}$], $L = 1340$. The fact that L is large (along with N large, required by the CLT) further impels S to be quite small, as (40b), for example, indicates. Figure 14 shows the estimated perform-

Authorized licensed use limited to: University of Missouri Libraries. Downloaded on April 02,2024 at 15:40:49 UTC from IEEE Xplore. Restrictions apply.

IPR2024-00817
Apple EX1035 Page 11

ance for the threshold receiver, from (40) and (42), along with the upper bound on the performance of the optimum detector calculated earlier for our case 0.35, $\Gamma' = 0.5 \times 10^{-3}$.

As Levin et al. [32] have pointed out, reliable detection when the signal is weak requires us to increase the sample size N. This leads to an increase in the effect of terms of higher order, which are discarded in the synthesis of locally optimal detectors. That is, for a given small signal level, the locally optimal detectors become increasingly suboptimum as N increases. This effect can be mitigated by using as a bias term $E(\ | H_{1,2})$ of the next-order terms in s_{1i}, s_{2i}, in the LOBD structures [25].

A few remarks are in order here regarding the effectiveness of such schemes. To determine this we need some useful criteria by which to compare the performance of optimum and the locally optimum detectors, particularly in the limiting situations of large sample size. The concepts of Relative Efficiency (RE) and Asymptotic Relative Efficiency (ARE) as proposed by Pitman [33] and specified in detail by Capon [34] and Middleton [25, 35], as well as others, provide the needed basis for comparison. For example, Middleton's generalized definitions are, for our case:

(i). The *Efficiency* of the test H_1 vs. H_2 by a system y with non-zero input signal intensity level ($S > 0$) and finite sample size N is, for a fixed P_e,

$$\epsilon_y(N, S) \equiv \left(\frac{\langle y_1 \rangle}{\sigma_1} - \frac{\langle y_2 \rangle}{\sigma_2} \right)^2, \tag{43a}$$

where $\langle y_1 \rangle$ denotes the mean of the test statistic y under hypothesis H_1, σ_1 the corresponding standard deviation, etc. Equations (40) and (41) allow us to calculate this quantity for our locally optimum detector.

(ii). The *Relative Efficiency* (RE) of the test H_1 vs H_2 by system y_1 vs. that by system y_2 is then

$$\epsilon_{y_1|y_2}(N_1, N_2, S) = \frac{\epsilon_{y_1}(N_1, S)}{\epsilon_{y_2}(N_2, S)}, \tag{43b}$$

where N_i, $i = 1,2$, is the sample size for system y_i for some required level of performance.

(iii). The *Asymptotic Relative Efficiency* (ARE) is, for given level S, given by

$$\lim_{N_1, N_2 \to \infty} \epsilon_{y_1|y_2}(N_1, N_2, S). \tag{43c}$$

If $\epsilon_{y_1|y_2}(N_1, N_2, S) \leqslant 1$, then y_2 is said to be more efficient than y_1, and if the ARE $\leqslant 1$, then y_2 is said to be asymptotically more efficient than y_1.

In our case, a more useful and equivalent relation is simply

$$\epsilon_{y_1|y_2}(N_1, N_2, S) = \frac{N_2}{N_1}. \tag{43d}$$

That is, the RE simply tells us [for a given small signal level S and required measure of performance P_e] how many more samples (N_1) system y_1 requires than the more efficient system y_2 (Levin and Kushnir [27]).

We have developed the means to obtain a good estimate of N_1 for any small signal size and required P_e for the locally optimum detector via (42). Obtaining N_2 (for the optimum detector), however, is not an easy matter, since all we have here is an upper bound, which is likely to be quite "loose" for small signal levels. However, we can apply a CLT argument to this upper bound to obtain an estimate of performance for the optimum detector, especially for small signals. This procedure is as follows: from Gallager [36], Appendix 5A, and Van Trees [13], Sec. 2.7, we let

$$\mu(\alpha) = \ln \int_{-\infty}^{\infty} [p(X) \mid H_1)]^{\alpha} [p(X) \mid H_2]^{1-\alpha} \, dX, \tag{44}$$

so that our bound (26), obtained earlier, is

$$P_e \leqslant \frac{1}{2} e^{\mu(\alpha^*)}, \tag{45}$$

where now α^* is the value of α for which $\dot{\mu}(\alpha) = 0$. In our case α^* was equal to 1/2, cf. (22). Then an estimate of performance, based on the CLT, is given (Van Trees, [13], Sec. 2.7) by

$$\begin{aligned} P_e \approx{} & \frac{1}{4} \exp \left[\mu(\alpha^*) + \frac{(\alpha^*)^2}{2} \ddot{\mu}(\alpha^*) \right] \operatorname{erfc} \frac{\alpha^* \sqrt{\ddot{\mu}(\alpha^*)}}{\sqrt{2}} \\ & + \frac{1}{4} \exp \left[\mu(\alpha^*) + \frac{(1-\alpha^*)^2}{2} \ddot{\mu}(\alpha^*) \right] \\ & \cdot \operatorname{erfc} \frac{(1-\alpha^*)\sqrt{\ddot{\mu}(\alpha^*)}}{\sqrt{2}}. \end{aligned} \tag{46}$$

Although (46) can be used then to obtain an estimate of N_2, it requires the computation of $\ddot{\mu}(\alpha^*)$. Direct differentiation of $\mu(\alpha)$ results in indeterminate forms for $\ddot{\mu}(\alpha^*)$ for our present case. Even so, the numerical evaluation of $\ddot{\mu}(\alpha^*)$, while rather involved, is straightforward. However, we are still left with estimates (hopefully good) of N_1 and N_2.

VI. CONCLUDING REMARKS (Part I)

Inasmuch as communications systems are seldom interfered with by "classical" white Gaussian noise, the principal objective of this paper (and Part II following) is to apply Middleton's recently developed statistical-physical model of "impulsive," highly non-Gaussian interference [4] to signal detection problems involving realistic electromagnetic interference environments. The new, canonical interference model used here is briefly described (the Class A noise case [4]) for the solution of these signal detection problems, and is shown to be in excellent agreement with experiment, as well.

In general, optimum and threshold optimum (LOBD)

Authorized licensed use limited to: University of Missouri Libraries. Downloaded on April 02,2024 at 15:40:49 UTC from IEEE Xplore. Restrictions apply.

IPR2024-00817
Apple EX1035 Page 12

detection algorithms are obtained, here canonically (i.e., independent of the type of interference) and for particular signal waveforms, for the situation of coherent binary detection, and in specific detail for three common digital signaling waveforms: i.e., antipodal, orthogonal, and ON-OFF keying. Quantitative performance bounds are also obtained for these specific signaling cases in Class A noise. It is well known that to gain significant improvement over current (matched-filter) receivers (in Gauss noise), the number of independent samples of the received interference waveform must be large. Performance measures are accordingly obtained which are explicitly parametric in sample-size, or equivalently in time-bandwidth product. Performance of the currently used, suboptimum (i.e., matched filter) receivers is also evaluated and compared with that of the optimum receiver in these highly non-Gaussian (Class A) noise environments. It is shown that substantial savings in signal power and/or spectrum space can be achieved if the proper optimum receivers are employed.

Although physical realizations of the completely optimum detection algorithms (for all signal levels) are not usually economically achievable, the corresponding locally optimum or threshold receiver (LOBD's) are derived and their performance evaluated. These threshold receiver-structures are canonical in nature in that the *form* of their structure is independent of the statistical character of the interference, and of particular signal waveforms.

In the present paper, all calculations of performance are carried out with the pdf of the interference in normalized form, cf. (7) and (9), so that the noise power is unity and the SNR is given by the signal power S. In actual situations, the performance of the optimum and locally optimum (LOBD) receivers is not a function of the SNR alone, because of the required nonlinear processing. That is, for problems of active interest, the performance algorithms developed here must use the pdf of the interference in unnormalized, or absolute form, so that performance (i.e., error probabilities) will, in general, depend on the absolute interference level as well as on the SNR. In this sense, then, these optimum receivers are also *adaptive;* i.e., they must be able to adjust to the parameters (level, Impulsive Index (A), etc.) of the interference.

Finally, Part II following extends the analysis to include various important types of incoherent reception.

REFERENCES

1. A. D. Spaulding, "Man-made noise: the problem and recommended steps toward solution", Office of Telecommunications, OT Report 76-85, April, 1976 (National Technical Information Service, U.S. Dep't of Commerce, Springfield, Va.).
2. D. Middleton, "Statistical-physical models of man-made radio noise, Part I: first-order probability models of the instantaneous amplitude", Office of Telecommunications, OT Report 74-36, April, 1974 (U.S. Gov. Printing Office, Wash., D.C. 20402).
3. A. D. Spaulding and D. Middleton, "Optimum reception in an impulsive interference environment," Office of Telecommunications, OT Report 75-67, June, 1975 (U.S. Gov't Printing Office, Wash., D.C., 20402).
4. D. Middleton, "Statistical-physical models of man-made and natural radio noise. Part II: first-order probability models of the envelope and phase", Office of Telecommunications, OT Report 76-86, April, 1976 (National Technical Information Service, U.S. Dep't. of Commerce, Springfield, Va.).
5. Middleton, D., A statistical theory of reverberation and similar first-order scattered fields; I, 372-392, II, 393-414; *IEEE trans. Info. Theory,* IT-13, No. 3, 1967.
6. Middleton, D., Statistical-physical models of urban radio-noise environments–Part I: Foundations, *IEEE Trans. on Electro. Comp.,* Vol. EMC-14, No. 2, 38-56, 1972.
7. Furutsu, K., and T. Ishida, On the theory of amplitude distribution of impulsive random noise and its application to the atmospheric noise, *Journal of the Radio Research Laboratories (Japan),* Vol. 7, No. 32, 1960.
8. Giordano, A. A., and F. Haber, Modeling of atmospheric noise, *Radio Science,* Vol. 7, No. 11, 1011-1023, 1972.
9. Adams, J. W., W. D. Bensema, and M. Kanda, Electro-magnetic noise Grace mine, National Bureau of Standards Report NBSIR 74-388, 1974.
10. Bolton, E. C., Simulating LF atmospheric radio noise and comparative characteristics of man-made and atmospheric radio noise at 60, 76, and 200 kHz, Office of Telecommunications Technical Memorandum OT TM-97 (available only from author), 1972.
11. Middleton, D., *An Introduction to Statistical Communication Theory* (McGraw-Hill Book Company, Inc., New York), 1960.
12. Hellman, M. E., and J. Raviv, Probability of error, equivocation, and the Chernoff bound, *IEEE trans. on Information Theory,* Vol. IT-16, No. 4, 368-372, 1970.
13. Van Trees, H. L., *Detection, Estimation, and Modulation Theory, Part I* (John Wiley and Sons, Inc., New York), 1968.
14. Hall, H. M., A new model for "impulsive" phenomena: Application to atmospheric noise communications channels, Stanford University Electronics Laboratories Technical Report No. 3412-8 and No. 7050-7, SU-SEL-66-052, 1966.
15. Spaulding, A. D., R. T. Disney, and L. R. Espeland, "Samso phase C–final report–noise data and analysis" (Hard Rock Silo Development, Program 12JB), ESSA/ITS ERLTM-ITS 184 (DDC, AD861428), 1969.
16. Miller, E. K., A variable interval width quadrature technique based on Romberg's method, *J. of Computational Physics,* 5, 265-279, 1970.
17. E. Conte, E. Corti, and F. Immirzi, "The characteristic function: a practical tool for the communication engineer", *Archiv. f. Elek. u. Ubertragungstechnik,* Vol. 29, p. 334-344, 1975.
18. E. Corti, F. Immirzi, M. Longo, and V. Vaccaro, "Error rates for fading PSK signals subject to generalized noise", *Archiv. f. Elek. u. Ubertragungstechnik,* Vol. 29, pp. 493-504, 1975.
19. Hancock, J. C., and P. W. Wintz, *Signal Detection Theory* (McGraw-Hill Book Company, New York, Chapter 3, 1966.
20. Arthurs, E., and H. Dym, On the optimum detection of digital signals–a geometric interpretation and a study of three basic data transmission systems, *IRE Trans. on Comm. Systems* (December), 336-372, 1962.
21. Halton, J. H., and A. D. Spaulding, Error rates in differentially coherent phase systems in non-Gaussian noise, *IEEE Trans. on Comm. Technology,* Vol. COM-14, No. 5, 594-601, 1966.
22. Mayer, R. J., Interference performance degradation to digital systems, *1972 IEEE International Electromagnetic Compatibility Symposium Record,* 97-104 (IEEE 72 CH0 638-7EMC), 1972.
23. Middleton, D., Statistical theory of signal detection, Symposium on Statistical Methods in Communications Engineering, *IRE Trans. on Information Theory,* PGIT-3:26, 1954.
24. Rudnick, P., Likelihood detection of small signals in stationary noise, *J. Appl. Phys.,* Vol. 32, 140-143, 1961.
25. Middleton, D., Canonically optimum threshold detection, *IEEE Trans. Information Theory,* Vol. IT-12, No. 2, 230-243, 1966.
26. Antonov, O. Y., Optimum detection of signals in non-Gaussian noise, *Radio Engr. and Electronic Phys.,* Vol. 12, 541-548, 1967.
27. Levin, B. R., and A. F. Kushnir, Asymptotically optimal algorithms of detection and extraction of signals from noise, *Radio Engr. and Electronic Phys.,* Vol. 14, No. 2, 213-221, 1970.
28. Levin, B. R., and Y. S. Shinakov, Asymptotic properties of Bayes estimates of parameters of a signal masked by interference, International Symposium on Information Theory, Noordwijk, The Netherlands, June 15-19, 1970.
29. Algazi, V. R., and M. Lerner, Binary detection in white, non-Gaussian noise, MIT Lincoln Labs Report LL/DS-2318, 1964. [See Letter to Editor, *Trans. Comm.,* Vol. COM-13, 1975, by Nirenberg and Middleton on the correct historical evolution of threshold detection techniques.]
30. Nirenberg, L. M., Low SNR digital communication over certain additive non-Gaussian channels, *IEEE Trans. on Comm.,* Vol.

Authorized licensed use limited to: University of Missouri Libraries. Downloaded on April 02,2024 at 15:40:49 UTC from IEEE Xplore. Restrictions apply.

IPR2024-00817
Apple EX1035 Page 13

COM-23, No. 3, 332-341, 1975. [See letter to Editor, *ibid.*, 1975, by Nirenberg and Middleton regarding the historical evolution of threshold detectors.]
31. Bernstein, S. L., and D. A. McNeill, An experimental ELF receiver, MIT Lincoln Labs Technical Report F19628-73-C-0002, ESD-TC-73-243 (September), 1973.
32. Levin, B. R., H. F. Kushnir, and A. I. Pinskiy, Asymptotically optimal algorithms for detection and discrimination of signals immersed in correlated noise, *Radio Engr. and Electronic Phys.*, Vol. 14, No. 2, 784-793, 1970.
33. Pitman, E. J. G., Lecture Notes on Nonparametric Statistical Interference, Columbia University, New York, 1948.
34. Capon, J., On the asymptotic efficiency of locally optimum detectors, *IRE Trans. Info. Theory*, Vol. IT-7 (April), 67-71, 1961.
35. Middleton, D., Canonically optimum threshold detection, The Rand Corp. Memorandum RM-4687-PR (NTIS AD626162), 1965.
36. Gallager, R. G., *Information Theory and Reliable Communication* (John Wiley and Sons, Inc., New York), 1968.

★

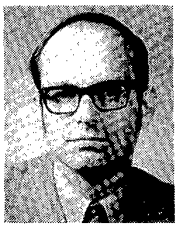

Arthur D. Spaulding is a mathematician with the Institute for Telecommunication Sciences. Born in Denver, Colorado, in 1935, he received the B.S.E.E. degree in 1957, the M.S. degree in Applied Mathematics in 1960, both from the University of Colorado, and the Ph.D. degree in E.E. from the University of Denver in 1975.

Dr. Spaulding joined the Tropospheric and Space Telecommunications Division of the Central Radio Propagation Laboratory, Boulder, Colorado, in 1957, where he worked on propagation and atmospheric radio noise prediction probelms. From 1958 to 1961 he was also an instructor in the Applied Mathematics Department at the University of Colorado. In 1961 he joined the Electromagnetic Interference Environment Program area of the Institute for Telecommunication Sciences, where he worked in the areas of statistical descriptions and predictions of interference and the analysis and design of systems operating in this interference. He is presently a member of the Radio Spectrum Occupancy Group of OT/ITS, where he is performing compatibility analyses and working in various areas of communication theory and detection processes.

Dr. Spaulding is a member of Eta Kappa Nu, Tau Beta Pi, Sigma Tau, and Sigma Xi. He has been active in the work of the CCIR, Study Groups 1 and 6, and the Technical Subcommittee of IRAC. Dr. Spaulding is the U.S. Chairman of Subgroup D of CCIR Study Group 6 and the U.S. member of CCIR International working Party 6/2. He is also a member of Commissions C and E of URSI and the U.S. Vice-Chairman of Commission E.

★

David Middleton (S'42-A'44-M'45-SM'53-F'59) is a Physicist, Applied Mathematician, and Educator. He was born in New York City on April 19, 1920. He received the A.B. (scl), A.M., and Ph.D. degrees from Harvard College in 1942, and Harvard University in 1945 and 1947 respectively.

He has been a Special Research Associate, Research Fellow, and Assistant Professor of Applied Physics at Harvard. He has also served as Adjunct Professor in Electrical Engineering and Applied Physics at Columbia University, Rensselaer Polytechnic Institute (Hartford Graduate Center), and currently, as well, at the University of Rhode Island; and as a visiting professor at the University of Texas. His general areas of research, teaching, and applications are principally (I) *Statistical Communication Theory* (with particular attention to random processes and signal detection and extraction theory (since 1942); (II) *Statistical Physics*—propagation and scatting in random media with emphasis on the underwater acoustic environment (since 1960); and (III) *Electromagnetic Compatibility*—models and processing for the man-made and natural electromagnetic environment (since 1968). Other areas of current interest are physical oceanography, remote sensing, optimal system design, and various special applications in communications, radar, and signal processing.

Dr. Middleton has published over 100 technical papers and two books in the above areas. His *Introduction to Statistical Communication Theory* (McGraw-Hill, 1960) and *Topics in Communication Theory* (McGraw-Hill, 1965) have also been published in translation by *Soviet Radio* (Moscow) 1961 and 1966. He is a consulting physicist and contractor with universities, industry, and various agencies of the Federal Government, including the Departments of Defense (Office of Naval Research), Commerce (Office of Telecommunications), and the Executive Office of the President (Office of Telecommunications Policy). He is currently a Member of the Naval Research Advisory Committee (NRAC), various advisory boards to NRAC, and other committees, such as CCIR (U.S. Study Group IE), and editorial advisory boards. He holds memberships and fellowships in many scientific and engineering societies, including Fellowship in the American Physical Society and American Association for the Advancement of Science (AAAS).

Authorized licensed use limited to: University of Missouri Libraries. Downloaded on April 02,2024 at 15:40:49 UTC from IEEE Xplore. Restrictions apply.

IPR2024-00817
Apple EX1035 Page 14